

# On the Metric Distortion of Embedding Persistence Diagrams into Reproducing Kernel Hilbert Spaces

Mathieu Carrière\* and Ulrich Bauer†

## Abstract

Persistence diagrams are important feature descriptors in Topological Data Analysis. Due to the nonlinearity of the space of persistence diagrams equipped with their *diagram distances*, most of the recent attempts at using persistence diagrams in Machine Learning have been done through kernel methods, i.e., embeddings of persistence diagrams into Reproducing Kernel Hilbert Spaces (RKHS), in which all computations can be performed easily. Since persistence diagrams enjoy theoretical stability guarantees for the diagram distances, the *metric properties* of a kernel  $k$ , i.e., the relationship between the RKHS distance  $d_k$  and the diagram distances, are of central interest for understanding if the persistence diagram guarantees carry over to the embedding. In this article, we study the possibility of embedding persistence diagrams into RKHS with bi-Lipschitz maps. In particular, we show that when the RKHS is infinite dimensional, any lower bound must depend on the cardinalities of the persistence diagrams, and that when the RKHS is finite dimensional, finding a bi-Lipschitz embedding is impossible, even when restricting the persistence diagrams to have bounded cardinalities.

## 1 Introduction

The increase of available data in both academia and industry have been exponential over the past few decades, making data analysis ubiquitous in many different fields of science. Machine Learning has proved to be one of the most prominent field of data science, leading to astounding results in various applications, such as image and signal processing. Topological Data Analysis (TDA) [Car09] is one specific field of Machine Learning, which focuses more on *complex* rather than big data. The general assumption of TDA is that data is actually sampled from geometric or low-dimensional domains, whose geometric features are relevant to the analysis. These geometric features are usually encoded in a mathematical object called *persistence diagram*, which is roughly a set of points in the plane, each point representing a topological feature whose size is contained in the coordinates of the point. Persistence diagrams have been proved to bring complementary information to other traditional descriptors in many different applications, often leading to large result improvements. This is also due to the so-called *stability properties* of the persistence diagrams, which state that persistence diagrams computed on similar data are also very close in the diagram distances [CSEH07, BL15, CdSGO16].

Unfortunately, the use of persistence diagrams in Machine Learning methods is not straightforward, since many algorithms expect data to be Euclidean vectors, while persistence diagrams are sets of points with possibly different cardinalities. Moreover, the *diagram distances* used to compare persistence diagrams are computed with optimal matchings, and thus quite different from Euclidean metrics. The usual way to cope with such difficult data is to use *kernel methods*. A kernel is a symmetric function on the data whose evaluation on a pair of data points equals the scalar product of the images of these points under a *feature map* into a Hilbert space, called the *Reproducing Kernel Hilbert Space* (RKHS) of the kernel. Both the feature map and the RKHS are usually not given explicitly. Many algorithms can be *kernelized*, such as PCA and SVM, allowing one to handle non-Euclidean data as soon as a kernel is available. Moreover, a seminal result in kernel methods states that the only requirement for a symmetric function to be a kernel is to be positive definite. Another possibility is to use Berg's theorem [BCR84], which states that a Gaussian computed with a given symmetric function is a kernel if the function is *conditionnally negative definite*.

---

\*mathieu.carriere@inria.fr

†ulrich.bauer@tum.de

Hence, the question of defining positive definite functions, i.e., kernels, for persistence diagrams has been intensively studied in the past few years, and, as of today, various kernels can be implemented, either into finite or infinite dimensional Hilbert spaces [Bub15, COO15, RHBK15, KFH16, AEK<sup>+</sup>17, CCO17, HKNU17]. Since persistence diagrams are known to enjoy stability properties, it is also natural to ask the same guarantee for their embeddings into a RKHS. Hence, all kernels defined in the literature satisfy a stability property stating that the RKHS distance between the image of the persistence diagrams is upper bounded by the diagram distances. A more difficult question is to prove whether a lower bound also holds or not. Even though one attempt has already been made to show such a lower bound for a Gaussian-like kernel in [CCO17], the question remains open in general.

**Contributions.** In this article, we tackle the general question of defining bi-Lipschitz embeddings of persistence diagrams into RKHS. More precisely, we show that:

- If such a bi-Lipschitz embedding exists, then either the lower bound goes to 0 or the upper bound goes to  $\infty$  as the number of points or their coordinates increase in the persistence diagrams (Theorem 3.2)
- Such a bi-Lipschitz embedding does not exist if the RKHS is finite dimensional (Theorem 3.6),

Finally, we also provide experimental evidence of this behavior by computing the metric distortion bounds of various persistence diagrams with increasing cardinalities.

**Related work.** Kernels for persistence diagrams can be classified into two different classes, depending whether the corresponding RKHS is finite or infinite dimensional.

In the infinite dimensional case, the first attempt was that proposed in [Bub15], in which persistence diagrams are turned into  $L^2$  functions, called Landscapes, by computing the homological rank functions given by the persistence diagram points. Another common way to define a kernel is to see the points of the persistence diagrams as centers of Gaussians with a fixed bandwidth, weighted by the distance of the point to the diagonal. This is the approach originally advocated in [RHBK15], and later generalized in [KFH17], leading to the so-called *Persistence Scale Space Kernel*. Another possibility is to define a Gaussian-like kernel by using the *Sliced Wasserstein distance* between persistence diagrams, which is conditionnally negative definite. This Gaussian-like kernel, called the *Sliced Wasserstein Kernel*, was defined in [CCO17].

In the finite dimensional case, many different possibilities are available. One may consider evaluating a family of tropical polynomials onto the persistence diagram [Ver16], taking the sorted vector of the pairwise distances between the persistence diagram points [COO15], or computing the coefficients of a complex polynomial whose roots are given by the persistence diagram points [dFF15]. Another line of work was proposed in [AEK<sup>+</sup>17] by discretizing the Persistence Scale Space Kernel. The idea is to discretize the plane into a fixed grid, and then compute a value for each pixel by integrating Gaussian functions centered on the persistence diagram points. Finally, persistence diagrams have been incorporated in deep learning frameworks in [HKNU17], in which Gaussian functions (whose means and variances are optimized by the neural network during training) are integrated against persistence diagrams seen as discrete measures.

## 2 Background

### 2.1 Persistence Diagrams

*Persistent homology* is a technique of TDA coming from topological algebra that allows the user to compute and encode topological information of datasets in a compact descriptor called the *persistence diagram* (persistence diagram). Given a dataset  $X$ , often given in the form of a point cloud in  $\mathbb{R}^n$ , and a continuous and real-valued function  $f : X \rightarrow \mathbb{R}$ , the persistence diagram of  $f$  can be computed under mild conditions (the function has to be *tame*, see [CdSGO16] for more details), and consists in a finite set of points with multiplicities in the upper-diagonal half-plane  $\text{Dg}(f) = \{(x_i, y_i)\} \subset \{(x, y) \in \mathbb{R}^2 : y > x\}$ . This set of points is computed from the family of *sublevel sets* of  $f$ , that is the sets of the form  $f^{-1}((-\infty, \alpha])$ , for some  $\alpha \in \mathbb{R}$ . More precisely, persistence diagrams encode the different *topological events* that occur as  $\alpha$  increases from  $-\infty$  to  $\infty$ . Such topological events include creation and merging of connected components and cycles in

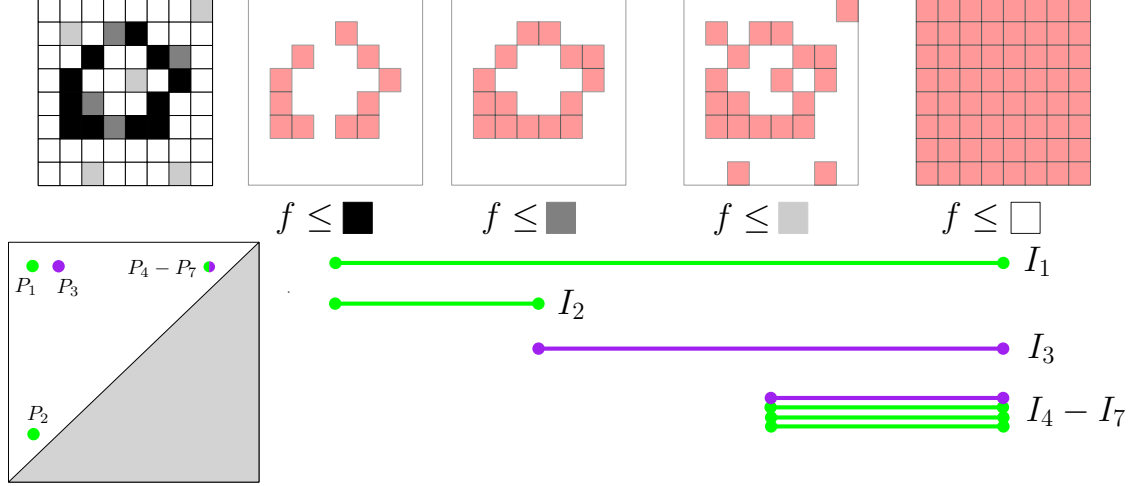


Figure 1: Example of persistence diagram computation. The space we consider is a blurry image of a zero, and the function  $f$  that we use is the grey level value on each pixel. We show four different sublevel sets of  $f$ . For each sublevel set, the corresponding pixels are displayed in pink color. In the first sublevel set, two connected components are present in the sublevel set, so we start two intervals  $I_1$  and  $I_2$ . In the second one, one connected component got merged to the other, so we stop the corresponding interval  $I_2$ , and a cycle (loop) is created, so we start a third interval  $I_3$ . In the third sublevel set, a new small cycle is created, as well as three more connected components. In the fourth sublevel set, all pixels belong to the set: all cycles are filled in and all connected components are merged together, so we stop all intervals. Finally, each interval  $I_k$  is represented as a point  $P_k$  in the plane (using the endpoints as coordinates).

every dimension. See Figure 1. Intuitively, persistent homology records, for each topological feature that appears in the family of sublevel sets, the value  $\alpha_b$  at which the feature appears, called the *birth value*, and the value  $\alpha_d$  at which it gets merged or filled in, called the *death value*. These values are then used as coordinates for a corresponding point in the persistence diagram. Note that several features may have the same birth and death values, so points in the persistence diagram have multiplicities. Moreover, since  $\alpha_d \geq \alpha_b$ , these points are always located above the diagonal  $\Delta = \{(x, x) : x \in \mathbb{R}\}$ . Another general intuition about persistence diagrams is that the distance of a point to  $\Delta$  is a direct measure of the point relevance: if a point is close to  $\Delta$ , it means that the corresponding cycle got filled in right after its appearance, thus suggesting that it is likely due to noise in the dataset. On the contrary, points that are far away from  $\Delta$  represent cycles with important sizes, and are more probably relevant for the analysis. We refer the interested reader to [EH10, Oud15] for more details about persistent homology.

**Notation.** Let  $\mathcal{D}$  be the space of persistence diagrams with finite number of points with finite coordinates. More formally,  $\mathcal{D}$  can be equivalently defined as a functional space  $\{m : \mathbb{R}^2 \setminus \Delta \rightarrow \mathbb{N} \text{ s.t. } |\text{supp}(m)| < \infty\}$ , where each point  $q \in \text{supp}(m)$  is a point in the corresponding persistence diagram with multiplicity  $m(q)$ . Let  $\mathcal{D}_N$  be the space of persistence diagrams with less than  $N$  points, i.e.,  $\mathcal{D}_N = \{m : \mathbb{R}^2 \setminus \Delta \rightarrow \mathbb{N} \text{ s.t. } \sum_q m(q) < N\}$ . Let  $\mathcal{D}^L$  be the space of persistence diagrams included in  $[-L, L]^2$ , i.e.,  $\mathcal{D}^L = \{m : \mathbb{R}^2 \setminus \Delta \rightarrow \mathbb{N} \text{ s.t. } \text{supp}(m) \subset [-L, L]^2\}$ . Finally, let  $\mathcal{D}_N^L$  be the space of persistence diagrams with less than  $N$  points included in  $[-L, L]^2$ , i.e.,  $\mathcal{D}_N^L = \mathcal{D}_N \cap \mathcal{D}^L$ . Obviously, we have the following sequences of (strict) inclusions:  $\mathcal{D}_N^L \subset \mathcal{D}_N \subset \mathcal{D}$ , and  $\mathcal{D}_N^L \subset \mathcal{D}^L \subset \mathcal{D}$ .

**Diagram distances.** Persistence diagrams can be efficiently compared using the *diagram distances*, which is a family of distances parametrized by an integer  $p$  that rely on the computation of *partial matchings*. Recall that two persistence diagrams  $\text{Dg}_1$  and  $\text{Dg}_2$  may have different number of points. A *partial matching*  $\Gamma$  between  $\text{Dg}_1$  and  $\text{Dg}_2$  is a subset of  $\text{Dg}_1 \times \text{Dg}_2$ . It comes along with  $\Gamma_1$  (resp.  $\Gamma_2$ ), which is the set of points of  $\text{Dg}_1$  (resp.  $\text{Dg}_2$ ) that are not matched to a point of  $\text{Dg}_2$  (resp.  $\text{Dg}_1$ ) by  $\Gamma$ . The  $p$ -cost of  $\Gamma$  is then computed as:

$$c_p(\Gamma) = \sum_{(p,q) \in \Gamma} \|p - q\|_\infty^p + \sum_{p \in \Gamma_1} \|p - \Delta\|_\infty^p + \sum_{q \in \Gamma_2} \|q - \Delta\|_\infty^p.$$

The  $p$ -diagram distance is then defined as the cost of the best partial matching:

**Definition 2.1.** *Given two persistence diagrams  $\text{Dg}_1$  and  $\text{Dg}_2$ , the  $p$ -diagram distance  $d_p$  is defined as:*

$$d_p(\text{Dg}_1, \text{Dg}_2) = \inf_\Gamma \sqrt[p]{c_p(\Gamma)}.$$

Note that in the literature, these distances are often called the *Wasserstein distances* between persistence diagrams. Here, we follow the denomination of [CCO17]. In particular, taking a maximum instead of a sum in the definition of the cost:

$$c_\infty(\Gamma) = \max_{(p,q) \in \Gamma} \|p - q\|_\infty + \max_{p \in \Gamma_1} \|p - \Delta\|_\infty + \max_{q \in \Gamma_2} \|q - \Delta\|_\infty.$$

allows to add one more distance in the family called the *bottleneck distance*:  $d_\infty(\text{Dg}_1, \text{Dg}_2) = \inf_\Gamma c_\infty(\Gamma)$ .

**Stability.** A useful property of persistence diagrams is *stability*. Indeed, it is well known in the literature that persistence diagrams computed from close functions are close themselves in the bottleneck distance:

**Theorem 2.2** ([CSEH07, CdSGO16]). *Given two tame functions  $f, g : X \rightarrow \mathbb{R}$ , one has the following inequality:*

$$d_\infty(\text{Dg}(f), \text{Dg}(g)) \leq \|f - g\|_\infty. \quad (1)$$

Note that stability results exist as well for the other diagram distances, but require more conditions—see [Oud15].

## 2.2 Kernel Methods

Kernel methods is a set of techniques that allows to handle data that not necessarily have a well-defined scalar product (such as persistence diagrams). The idea is to send the data in a specific Hilbert space called *Reproducing Kernel Hilbert Space* (RKHS), and to use its corresponding scalar product.

**Definition 2.3.** *Let  $X$  be a set, and  $\mathcal{H} \subset \mathbb{R}^X$  be a Hilbert space. Then  $\mathcal{H}$  is a RKHS if and only if the mapping  $\begin{cases} \mathcal{H} & \rightarrow \mathbb{R} \\ f & \mapsto f(x) \end{cases}$  is continuous for any  $x \in X$ .*

Then, due to Riesz representation theorem, there exists  $k_x \in \mathcal{H}$  such that  $f(x) = \langle f, k_x \rangle_{\mathcal{H}}$ . The function  $\Phi : x \mapsto k_x$  is called the *feature map*, and the symmetric function  $k(x, y) = \langle k_x, k_y \rangle_{\mathcal{H}}$  is called the *kernel* of  $\mathcal{H}$ . Reciprocally, it can be shown that a symmetric function is the kernel of at most one RKHS. Scalar products and distances can be easily computed in  $\mathcal{H}$  with

$$\langle k_x, k_y \rangle_{\mathcal{H}} = k(x, y)$$

(which is called the reproducing property of  $\mathcal{H}$ ) and

$$\|k_x - k_y\|_{\mathcal{H}}^2 = \langle k_x - k_y, k_x - k_y \rangle_{\mathcal{H}} = k(x, x) + k(y, y) - 2k(x, y).$$

Moreover, it is very easy to characterize symmetric functions that are actually kernels thanks to the following result:

**Theorem 2.4.** *Let  $X$  be a set. Given a symmetric function  $k : X \times X \rightarrow \mathbb{R}$ , there exists a corresponding RKHS (i.e.,  $k$  is a kernel) if and only if  $k$  is positive definite:  $\sum_{i,j} a_i a_j k(x_i, x_j) \geq 0$  for any  $a_1, \dots, a_n \in \mathbb{R}$  and  $x_1, \dots, x_n \in X$ .*

Finally, Schönberg's theorem [BCR84] is very useful to define Gaussian-like kernels:

**Theorem 2.5.** *Let  $X$  be a set, and  $d : X \times X \rightarrow \mathbb{R}$  a symmetric function. Then the Gaussian  $k(x, x') = \exp(-d(x, x')/2\sigma^2)$  is a kernel for all  $\sigma > 0$  if and only if  $d$  is conditionally negative definite, i.e.,  $\sum_{i,j} a_i a_j d(x_i, x_j) \leq 0$  for any  $x_1, \dots, x_n \in X$  and  $a_1, \dots, a_n \in \mathbb{R}$  such that  $\sum_i a_i = 0$ .*

Note that  $d$  needs not be a metric. Note also that, given a kernel  $k$  on a set  $X$ , the square of the corresponding RKHS distance  $d_k^2$  is always conditionally negative definite. Indeed, let  $x_1, \dots, x_n \in X$  and  $a_1, \dots, a_n \in \mathbb{R}$  whose sum is zero. Then we have the following equalities:

$$\sum_{i,j} a_i a_j d_k^2(x_i, x_j) = \sum_{i,j} a_i a_j (k(x_i, x_i) + k(x_j, x_j) - 2k(x_i, x_j)) = -2 \sum_{i,j} a_i a_j k(x_i, x_j) \leq 0,$$

since  $\sum_i a_i = 0$  and  $k$  is positive definite.

We now provide some background results about Hilbert spaces. To begin with, the following theorem characterizes unit balls in Hilbert spaces, which will be useful for the analysis of a RKHS constructed in Section 3.1.

**Theorem 2.6** (Banach-Alaoglu). *The unit ball in a Hilbert space is weakly compact. In other words, for any sequence  $(v_n)$  such that  $\|v_n\| \leq 1$  for all  $n \in \mathbb{N}$ , there exists  $v \in \mathcal{H}$  and an increasing  $\psi : \mathbb{N} \rightarrow \mathbb{N}$  such that  $\|v\| \leq 1$ , and  $\langle u, v_{\psi(n)} \rangle \rightarrow \langle u, v \rangle$  for any  $u \in \mathcal{H}$ . If, in addition, we have  $\|v_{\psi(n)}\| \rightarrow \|v\|$ , then the convergence is strong:  $\|v_{\psi(n)} - v\| \rightarrow 0$ .*

Specifically, we use this result to show that a certain non-compact set of persistence diagrams would have to be mapped to a compact set by any bi-Lipschitz map to a Hilbert space, which is impossible since bi-Lipschitz maps preserve compactness. In order to carry out the argument, we use the following results, which allow us to work with an orthonormal basis of a RKHS.

**Theorem 2.7** (Mercer, see Theorem 3.a.1 in [Kön86]). *Let  $(X, \mu)$  be a finite measure space, and  $k : X \times X \rightarrow \mathbb{R}$  be a bounded kernel in  $L_\infty(X \times X, \mu \times \mu)$ , with corresponding RKHS  $\mathcal{H}$ . Then there exists  $\{u_i\}_{i \in \mathbb{N}} \subset L^2(X, \mu)$  s.t.*

$$k(x, x') = \sum_{i=0}^{\infty} u_i(x) u_i(x'), \quad (2)$$

where the convergence is in  $L_\infty(X \times X, \mu \times \mu)$ .

More can be said of the family  $\{u_i\}_{i \in \mathbb{N}}$ , provided that (2) converges *everywhere* (and not only almost everywhere):

**Proposition 2.8** (Theorem 3.1 in [SS12]). *If (2) converges pointwise everywhere, then  $\{u_i\}_{i \in \mathbb{N}}$  is an orthonormal basis of  $\mathcal{H}$ .*

## 2.3 Bi-Lipschitz embeddings

The main question that we address in this article is the one of preserving the persistence diagram properties when using kernels. For instance, one may ask the images of the persistence diagrams under the feature map to be stable as well in the RKHS distance. This is the case for *stable* kernels, which satisfy  $d_k(\Phi(\text{Dg}), \Phi(\text{Dg}')) \leq C d_p(\text{Dg}, \text{Dg}')$  for some  $p \in \mathbb{N} \cup \{\infty\}$  and constant  $C > 0$ . For instance, many kernels in the literature such as the Persistence Scale Space Kernel and the Sliced Wasserstein Kernel, are stable w.r.t. the first diagram distance  $d_1$ . A natural question is then whether a lower bound also holds, i.e., whether the feature map  $\Phi$  is a *bi-Lipschitz embedding* between  $(\mathcal{D}, d_p)$  and  $(\mathcal{H}, d_k)$ .

**Definition 2.9.** *Let  $(X, d_X)$  and  $(Y, d_Y)$  be two metric spaces. A bi-Lipschitz embedding between  $(X, d_X)$  and  $(Y, d_Y)$  is a map  $\Phi : X \rightarrow Y$  such that there exist constants  $0 < A, B < \infty$  such that:*

$$A d_X(x, x') \leq d_Y(\Phi(x), \Phi(x')) \leq B d_X(x, x'),$$

for any  $x, x' \in X$ . The metrics  $d_X$  and  $d_Y$  are called strongly equivalent, and the constants  $A$  and  $B$  are called the lower and upper metric distortion bounds respectively. If  $A = B$ ,  $\Phi$  is called an isometric embedding.

For example, the Sliced Wasserstein Kernel [CCO17] was constructed using Theorem 2.5 by defining a conditionally negative definite metric between persistence diagrams called the *Sliced Wasserstein distance* that is strongly equivalent to the first diagram distance  $d_1$  on  $\mathcal{D}_N^L$ . However, the lower metric distortion bound goes to 0 quadratically as  $N$  increases. In the following section, we study the behavior of the metric distortion bounds for kernels in general.

Note also that finding an isometric embedding of persistence diagrams into a RKHS is impossible since geodesics are unique in a Hilbert space while this is not the case for persistence diagrams, as shown in the proof of Proposition 2.4 in [TMMH14].

### 3 Metric Distortion Bounds

In this section, we prove our main results —Theorem 3.2 and Theorem 3.6—about the embeddings of persistence diagrams into RKHS. Even if these results extend freely to embeddings into general Hilbert spaces, we state them in the framework of RKHS since it is the main application of persistence diagram embeddings in Machine Learning.

#### 3.1 Infinite dimensional RKHS

In order to show our first main result Theorem 3.2, we first provide the following lemma, which relates the metric distortion bounds computed on  $\mathcal{D}_N^L$ ,  $\mathcal{D}^L$ ,  $\mathcal{D}_N$  and  $\mathcal{D}$ .

**Lemma 3.1.** *Let  $p \in \mathbb{N}$  and let  $d$  be a metric on persistence diagrams such that  $d$  is continuous w.r.t.  $d_p$  on  $\mathcal{D}$ . Let  $R_N^L = \{d_p(\text{Dg}, \text{Dg}')/d(\text{Dg}, \text{Dg}') : \text{Dg} \neq \text{Dg}' \in \mathcal{D}_N^L\}$ , let  $A_N^L = \inf R_N^L$  and  $B_N^L = \sup R_N^L$ .*

*Since  $A_N^L$  is nonincreasing and  $B_N^L$  is nondecreasing w.r.t.  $N$  and  $L$ , we define:*

$$A_N = \lim_{L \rightarrow +\infty} A_N^L, \quad B_N = \lim_{L \rightarrow +\infty} B_N^L, \quad A^L = \lim_{N \rightarrow +\infty} A_N^L, \quad B^L = \lim_{N \rightarrow +\infty} B_N^L$$

*Then the following inequalities hold:*

$$A^L d(\text{Dg}, \text{Dg}') \leq d_p(\text{Dg}, \text{Dg}') \leq B^L d(\text{Dg}, \text{Dg}'), \quad \text{and} \quad A_N d(\text{Dg}, \text{Dg}') \leq d_p(\text{Dg}, \text{Dg}') \leq B_N d(\text{Dg}, \text{Dg}')$$

*where  $\text{Dg}, \text{Dg}'$  belong to  $\mathcal{D}^L$ ,  $\mathcal{D}_N$  and  $\mathcal{D}$  respectively. Note that  $A_N$ ,  $A^L$ ,  $B_N$  and  $B^L$  may be equal to 0 or  $\infty$ , so these inequalities do not necessarily mean that  $d$  and  $d_p$  are strongly equivalent on  $\mathcal{D}_N$ ,  $\mathcal{D}^L$  or  $\mathcal{D}$ .*

We now show our first main result, which states that, given a kernel  $k$  for persistence diagrams, if the induced distance  $d_k$  in its corresponding RKHS is strongly equivalent to a diagram distance on  $\mathcal{D}_N^L$ , then at least one of the two metric distortion bounds depends on the persistence diagrams, and goes to either 0 or  $\infty$  as  $N$  or  $L$  increases.

**Theorem 3.2.** *Let  $p \in \mathbb{N} \cup \{\infty\}$  and  $d_p$  be the corresponding diagram distance. Let  $k$  be a continuous kernel on persistence diagrams, and let  $d_k$  be the corresponding RKHS distance. Assume that for any  $N \in \mathbb{N}$  and  $L > 0$ , there exist  $0 < A_N^L, B_N^L < \infty$  such that, for any  $\text{Dg}, \text{Dg}' \in \mathcal{D}_N^L$ :*

$$A_N^L d_k(\text{Dg}, \text{Dg}') \leq d_p(\text{Dg}, \text{Dg}') \leq B_N^L d_k(\text{Dg}, \text{Dg}').$$

*Then  $\frac{B_N^L}{A_N^L} \rightarrow \infty$  when  $L$  is fixed and  $N \rightarrow \infty$ , or when  $N$  is fixed and  $L \rightarrow \infty$ .*

*Proof.* We first prove the result when  $N \rightarrow \infty$ , and we fix some  $L > 0$ . According to Lemma 3.1, all we have to show is that  $d_k$  and  $d_p$  are not strongly equivalent on  $\mathcal{D}^L$ . We proceed by contradiction and assume that they are. In particular, this means that any space which is compact with one metric should also be compact with the other. Hence, the idea of the proof is to reach a contradiction by constructing a space  $X \subset \mathcal{D}^L$  which is provably compact with  $d_k$  but not with  $d_p$ .

Let us define this space  $X$  as follows:  $X = \{\text{Dg}_n\}_{n \in \mathbb{N}}$ , where  $\text{Dg}_n = \sqcup_{i=1}^n \{q\}$  and  $q = (-L, L) \in \mathbb{R}^2$ . Hence,  $X$  is a discrete metric space for which the distance  $d_p$  between any two elements is larger than  $L$ . Indeed, this distance is obtained by matching  $|j - i|$  replicates of  $q$  to the diagonal, so  $d_p(\text{Dg}_i, \text{Dg}_j) = L|j - i|^{\frac{1}{p}} \geq L$ . As such,  $X$  is complete and not compact when equipped with  $d_p$ .

We will prove that  $X$  is compact w.r.t.  $d_k$ , contradicting the assumption that  $d_k$  and  $d_p$  are equivalent. The idea is to define a Gaussian kernel  $G$  on  $X$  with Theorem 2.5, using the fact that  $d_k^2$  is conditionally negative definite. Since the image of the feature map of  $G$  is in the unit sphere of its RKHS, we can then use Theorem 2.6 to show that this image is weakly compact with the RKHS distance, which can then be used to show that  $X$  is compact with  $d_k$ .

More formally, define  $G(\cdot, \cdot) = \exp(-d_k^2(\cdot, \cdot))$ . Then  $G$  is a kernel on  $X \times X$ , with corresponding RKHS  $\mathcal{H}$ . Moreover,  $G$  is bounded on  $X$  since  $G(\cdot, \cdot) \leq 1$ . Hence, according to Theorem 2.7, there exists a family  $\{u_i\}_{i \in \mathbb{N}}$  such that  $G(\cdot, \cdot) = \sum_{i=0}^{\infty} u_i(\cdot) u_i(\cdot)$ , where the convergence is in  $L_{\infty}(X \times X, \mu \times \mu)$ . We now equip  $X$  with a positive measure  $\mu$ , defined on each singleton with  $\mu(\{Dg_n\}) = \exp(-n)$ . In particular, we have  $\mu(X) = \sum_{i=1}^{\infty} \exp(-i) < \infty$ . Moreover, since  $\mu(\{Dg_n\})$  is positive for all  $n \in \mathbb{N}$ , there is no non empty  $S \subseteq X$  with  $\mu(S) = 0$ , and thus  $L_{\infty}(X \times X, \mu \times \mu)$  convergence means uniform and pointwise convergence on  $X \times X$ . Hence,  $\{u_i\}_{i \in \mathbb{N}}$  is also an orthonormal basis of  $\mathcal{H}$  by Proposition 2.8.

We now show that  $X$  is compact w.r.t.  $d_k$ . Let  $\Phi : X \rightarrow \mathcal{H}$  be the feature map induced by  $G$ . Then  $\Phi(X)$  is included in the unit sphere of  $\mathcal{H}$  since  $\|\Phi(Dg_n)\|_{\mathcal{H}}^2 = G(Dg_n, Dg_n) = 1$ . According to Theorem 2.6, there exists an increasing  $\psi : \mathbb{N} \rightarrow \mathbb{N}$  such that the sequence  $\Phi(Dg_{\psi(n)})$  weakly converges to some  $u \in \mathcal{H}$  with  $\|u\|_{\mathcal{H}} \leq 1$ . We have the following equalities:

$$\begin{aligned}
1 &= \lim_{n \rightarrow +\infty} \|\Phi(Dg_{\psi(n)})\|_{\mathcal{H}}^2 = \lim_{n \rightarrow +\infty} \sum_{i=0}^{\infty} u_i(Dg_{\psi(n)})^2 \\
&= \sum_{i=0}^{\infty} \lim_{n \rightarrow +\infty} u_i(Dg_{\psi(n)})^2 && \text{(uniform convergence)} \\
&= \sum_{i=0}^{\infty} \lim_{n \rightarrow +\infty} \langle u_i, \Phi(Dg_{\psi(n)}) \rangle_{\mathcal{H}}^2 && \text{(reproducing property)} \\
&= \sum_{i=0}^{\infty} \langle u_i, u \rangle_{\mathcal{H}} && \text{(weak convergence of } \Phi(Dg_{\psi(n)})) \\
&= \|u\|_{\mathcal{H}}^2 && (\{u_i\}_{i \in \mathbb{N}} \text{ is an orthonormal basis)}
\end{aligned}$$

Finally, since  $\Phi(Dg_{\psi(n)})$  weakly converges to  $u$  and  $\|\Phi(Dg_{\psi(n)})\|_{\mathcal{H}}$  converges to  $\|u\|_{\mathcal{H}}$ , it follows that  $\Phi(Dg_{\psi(n)})$  strongly converges to  $u$  by Theorem 2.6, and thus is Cauchy w.r.t.  $\|\cdot\|_{\mathcal{H}}$ . Since  $X$  is complete w.r.t.  $d_p$ , and since  $d_k$  is strongly equivalent to  $d_p$  by assumption, it follows that  $X$  is also complete w.r.t.  $d_k$ . This means that  $\Phi(X)$  is complete w.r.t.  $\|\cdot\|_{\mathcal{H}}$  by the following equalities:

$$\|\Phi(Dg_n) - \Phi(Dg_m)\|_{\mathcal{H}}^2 = k(Dg_n, Dg_n) + k(Dg_m, Dg_m) - 2k(Dg_n, Dg_m) = 2(1 - \exp(-d_k^2(Dg_n, Dg_m))).$$

Hence there exists  $Dg \in X$  such that  $u = \Phi(Dg)$  and  $Dg_{\psi(n)}$  converges to  $Dg$  w.r.t.  $d_k$  and  $d_p$ . In particular, this means that  $X$  is compact w.r.t.  $d_k$ .

Since the same proof applies when  $X$  is replaced by  $Y = \{Dg'_n\}_{n \in \mathbb{N}}$  where  $Dg'_n = \{(0, n)\}$ , it follows that  $d_k$  and  $d_p$  are also not strongly equivalent on  $\mathcal{D}_N$ , and thus that the result also holds when  $L \rightarrow \infty$ .  $\square$

### 3.2 Finite dimensional RKHS

In our second main result, we show that more can be said about feature maps into  $\mathbb{R}^n$  (equipped with the Euclidean metric), using the so-called *Assouad dimension*.

**Assouad dimension.** The following definition and example are taken from paragraph 10.13 of [Hei01].

**Definition 3.3.** Let  $(X, d_X)$  be a metric space. Given a subset  $E \subset X$  and  $r > 0$ , let  $N_r(E)$  be the least number of open balls of radius less than or equal to  $r$  that can cover  $E$ . The Assouad dimension of  $X$  is:

$$\dim_A(X, d_X) = \inf\{\alpha > 0 : \exists C > 0 \text{ s.t. } \sup_{x \in X} N_{\beta r}(B(x, r)) \leq C\beta^{-\alpha}, \forall r > 0, \beta \in (0, 1]\}.$$

Intuitively, the Assouad dimension measures the number of open balls needed to cover an open ball of larger radius. It is a *fractal dimension*, and may be equal to  $\infty$ .

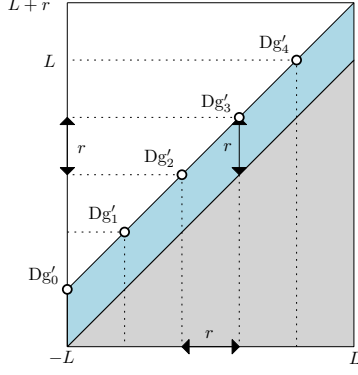


Figure 2: Persistence diagram used in the proof of Lemma 3.5. In this particular example, we have  $M = 5$ .

**Example.** The Assouad dimension of  $\mathbb{R}^n$  is  $n$ .

**Proposition 3.4** (Lemma 9.6 in [Rob10]). *Let  $(X, d_X)$  and  $(Y, d_Y)$  be metric spaces with a bi-Lipschitz embedding  $\Phi : X \rightarrow Y$ . Then  $\dim_A(X, d_X) = \dim_A(\text{im}(\Phi), d_Y)$ .*

**Non-embeddability.** We now show that  $\mathcal{D}_N^L$  cannot be embedded into  $\mathbb{R}^n$  with bi-Lipschitz embeddings. The proof of this fact is a consequence of the following lemma:

**Lemma 3.5.** *Let  $p \in \mathbb{N} \cup \{\infty\}$ ,  $N \in \mathbb{N}$ , and  $L > 0$ . Then  $\dim_A(\mathcal{D}_N^L, d_p) = \infty$ .*

*Proof.* Let  $B_p$  denote an open ball with  $d_p$ . We want to show that, for any  $\alpha > 0$  and  $C > 0$ , it is possible to find a persistence diagram  $\text{Dg} \in \mathcal{D}_N^L$ , a radius  $r > 0$  and a factor  $\beta \in (0, 1]$  such that the number of open balls of radius at most  $\beta r$  needed to cover  $B_p(\text{Dg}, r)$  is strictly larger than  $C\beta^{-\alpha}$ . To this end, we pick arbitrary  $\alpha > 0$  and  $C > 0$ . The idea of the proof is to define  $\text{Dg}$  as the empty diagram, and to derive a lower bound on the number of balls with radius  $\beta r$  needed to cover  $B_p(\text{Dg}, r)$  by considering persistence diagrams with one point evenly distributed on the line  $\{(x, x+r) : x \in [-L, L]\}$  such that the distance between two consecutive points is  $r$  in the  $\ell_\infty$ -distance. Indeed, the pairwise distance between any two such persistence diagrams is sufficiently large so that they must belong to different balls. Then we can control the number of persistence diagrams, and thus the number of balls, by taking  $r$  sufficiently small.

More formally, let  $M = 1 + \lfloor C\beta^{-\alpha} \rfloor > C\beta^{-\alpha}$ . We want to show that we have at least  $M$  balls in the cover, meaning that  $|\{\text{Dg}_i\}| \geq M$ . Let  $r = 2L/M$  and  $\beta = \frac{1}{2}$ . We define a cover of  $B_p(\text{Dg}, r)$  with open balls of radius less than  $\beta r$  centered on a family  $\{\text{Dg}_i\}$  as follows:

$$B_p(\text{Dg}, r) \subseteq \bigcup_i B_p(\text{Dg}_i, \beta r). \quad (3)$$

We now define particular persistence diagrams which all lie in different elements of the cover (3). For any  $0 \leq j \leq M-1$ , we let  $\text{Dg}'_j$  denote the persistence diagram containing only the point  $(-L+jr, -L+(j+1)r)$ . It is clear that each  $\text{Dg}'_j$  is in  $\mathcal{D}_N^L$ . See Figure 2.

Moreover, since  $d_p(\text{Dg}, \text{Dg}'_j) = \frac{r}{2} < r$ , it also follows that  $\text{Dg}'_j \in B_p(\text{Dg}, r)$ .

Hence, according to (3), for each  $j$  there exists an integer  $i_j$  such that  $\text{Dg}'_j \in B_p(\text{Dg}_{i_j}, \beta r)$ . Finally, note that  $j \neq j' \Rightarrow i_j \neq i_{j'}$ . Indeed, assuming that there are  $j \neq j'$  such that  $i_j = i_{j'}$ , and since the distance between  $\text{Dg}'_j$  and  $\text{Dg}'_{j'}$  is always obtained by matching their points to the diagonal, we reach a contradiction with the following application of the triangle inequality:

$$d_p(\text{Dg}'_j, \text{Dg}'_{j'}) = 2^{\frac{1}{p}} \frac{r}{2} \leq d_p(\text{Dg}'_j, \text{Dg}_{i_j}) + d_p(\text{Dg}_{i_j}, \text{Dg}_{i_{j'}}) + d_p(\text{Dg}_{i_{j'}}, \text{Dg}'_{j'}) < 2\beta r = r.$$

This observation shows that there are at least  $M$  different open balls in the cover (3), which concludes the proof.  $\square$

The following theorem is then a simple consequence of Lemma 3.5 and Proposition 3.4:



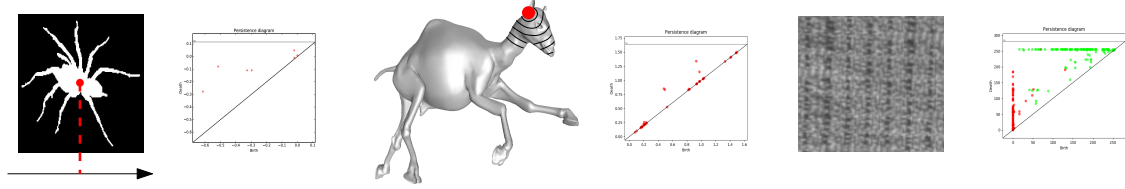


Figure 3: Example of persistence diagrams from the three datasets. On the left, we show an example of spider image together with its persistence diagram computed from the x-coordinate function defined on the white pixels. In the middle, we show the 3D shape representing a camel and a red point sampled on the shape. We also show few levelsets of the geodesic distance function to this point and its corresponding persistence diagram. Finally, we present an example of texture image and its associated persistence diagram computed with the CLBP-S descriptor on the right (red and green colors mean homological dimension 0 and 1 respectively).

**Theorem 3.6.** *Let  $p \in \mathbb{N} \cup \{\infty\}$  and  $n \in \mathbb{N}$ . Then, for any  $N \in \mathbb{N}$  and  $L > 0$ , there is no bi-Lipschitz embedding between  $(\mathcal{D}_N^L, d_p)$  and  $\mathbb{R}^n$ .*

Interestingly, the integers  $N$  and  $n$  are independent in Theorem 3.6: even if one restricts to persistence diagrams with only one point, it is still impossible to find a bi-Lipschitz embedding into  $\mathbb{R}^n$ , whatever  $n$  is.

## 4 Experiments

In this section, we compute metric distortions for various persistence diagrams in order to observe experimentally the behavior proved in the previous sections. Since most kernels are theoretically stable w.r.t. the first diagram distance, we compare  $d_1$  and the distances  $d_k$  induced by various kernels for persistence diagrams, namely:

- the distance induced by the Persistence Scale Space Kernel with  $\sigma = 1$  [RHBK15],
- the  $L^2$  distance between the first 10 Landscapes [Bub15],
- the Sliced Wasserstein distance [CCO17],
- the Euclidean distance between Persistence Vectors truncated to 100 dimensions [COO15],
- the Euclidean distance between discretizations of the Persistence Weighted Gaussian Kernel [KFH17], called the Persistence Images [AEK<sup>+</sup>17], computed on a  $50 \times 50$  grid with  $\sigma = 100$  and arctan weighting function with  $C = p = 1$ .

**Uniform sampling.** In our first experiment, we generated 30 persistence diagrams with points uniformly sampled in the upper half-square  $\{(x, y) : -10 \leq x \leq y \leq 10\}$ . We then computed metric distortion bounds for persistence diagram cardinalities increasing from 10 to 4000. For each cardinality, we show the logarithm of the ratio between the upper and lower metric distortion bounds in Figure 4. According to Theorem 3.2, since all kernels are stable, meaning that the upper metric distortion bound is constant, the lower metric distortion bound has to go to zero, and thus the ratio between them should diverge. As one can easily see, there is a clear increase with the cardinality of the persistence diagrams. However, the increase speed is different from a kernel to another. In particular, the Landscapes and Persistence Vectors seem to diverge rather fast.

**Existing datasets.** In our second experiment, we computed distributions of ratios between the diagram distances and the kernel distances for three persistence diagram datasets that have been used in TDA for various classification tasks. Since we are now looking at the ratio between the distances instead of the metric distortion bounds, the distribution values should decrease with the cardinalities.

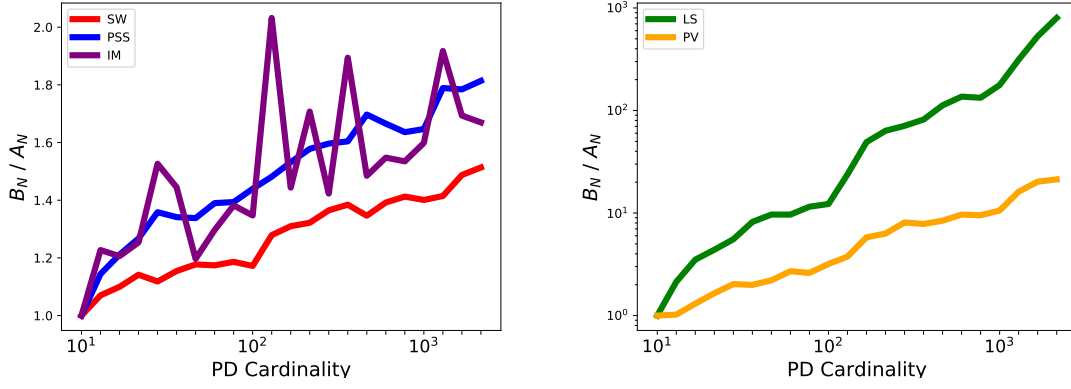


Figure 4: Plot of the ratio between the empirical upper and lower metric distortion bounds versus persistence diagram cardinalities for various kernels. Left: the Sliced Wasserstein Kernel (red), the Persistence Scale Space Kernel (blue) and the Persistence Images (purple). Right: the Landscapes (green) and Persistence Vectors (orange).

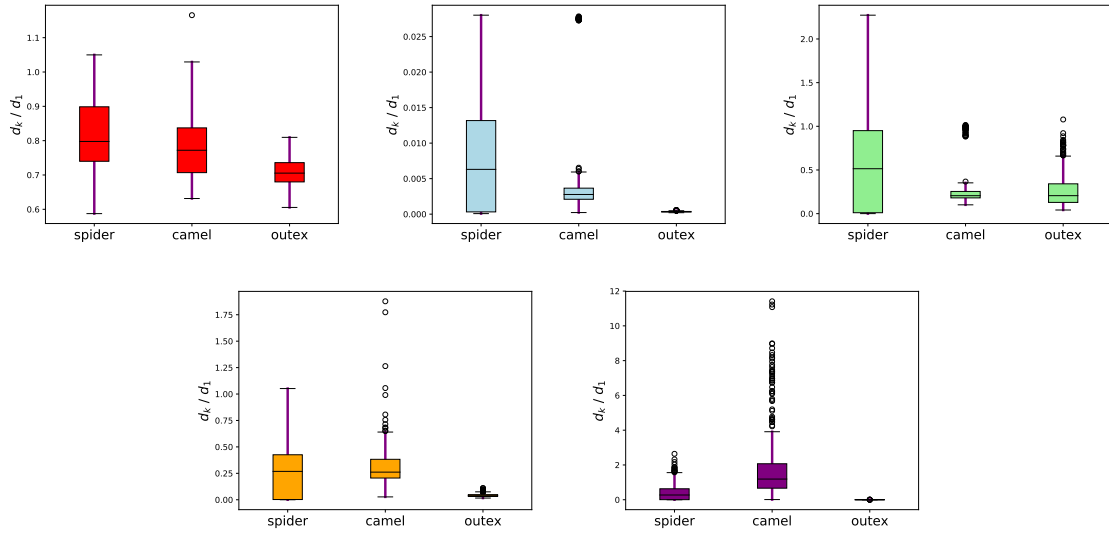


Figure 5: Boxplots of the empirical metric distortion between the first diagram distance  $d_1$  and various kernel distances. From left to right and top to bottom: the Sliced Wasserstein distance (red), the Persistence Scale Space distance (blue), the Landscapes (green), the Euclidean distance for Persistence Vectors (orange) and the Euclidean distance for Persistence Images (purple). There is a clear decrease in the distortion due to the increase in the cardinalities of persistence diagrams from the outex dataset.

The first dataset ("spider") is the spider category of the binary images dataset introduced in [BLT09]. The procedure used to compute persistence diagrams is taken from [HKNU17], and requires the sublevel sets of the x-coordinate function. For each image  $I = W \cup B$  composed of white and black pixels, we compute  $\text{Dg}(f_x)$ , where  $f_x : W \rightarrow \mathbb{R}$ , which is defined over the white pixels, is simply the pixel abscissa. Persistence diagrams in this dataset have 10 points in average.

The second one ("camel") is the first 3D shape representing a camel in the shape dataset introduced in [SP04]. The procedure used to compute persistence diagrams is taken from [COO15], and requires the sublevel sets of the geodesic distance function from various points sampled on this 3D shape  $S$ . More precisely, we randomly sample 30 points on  $S$ , and for each sampled point  $p \in S$ , we compute  $\text{Dg}(f_p)$ , where  $f_p : S \rightarrow \mathbb{R}$  is the geodesic distance to  $p$ . Persistence diagrams in this datasets have 40 to 50 points in average.

The third one ("outex") is the texture image dataset introduced in [OMP<sup>+</sup>02]. The procedure used to compute persistence diagrams is taken from [RHBK15], and is obtained with the sublevel sets of the CLBP descriptor on various images representing textures. We first subsample the data to  $32 \times 32$  images, and for each image, we compute  $\text{Dg}(f)$ , where  $f : I \rightarrow \mathbb{R}$  is the rotation-invariant version of the CLBP-S descriptor with radius  $R = 1$  and  $N = 8$  neighbors [GZZ10]. Persistence diagrams in this datasets have 100 to 200 points in average.

See Figure 3 for examples of persistence diagrams in each dataset. For each dataset, we computed boxplots on the distributions of distance ratios of the different kernels. As one can see from Figure 5, there is a clear decrease in the distribution values when going from spider and camel datasets to outex dataset, which is again due to the increase in the persistence diagram cardinalities.

## 5 Conclusion

In this article, we provided two important theoretical results about the use of persistence diagrams in Machine Learning. Most of the recent attempts have defined kernels for persistence diagrams and showed they were stable w.r.t. the diagram distances, and conjectured whether a lower bound holds as well or not. In this work, we prove that this is never the case if the kernel is finite dimensional, and that such a lower bound has to go to zero with the number of points if the kernel is infinite dimensional. We also provided experiments that confirm this result, by showing a fast decrease of the metric distortion with the number of points for persistence diagrams generated either synthetically or from real-world datasets.

## References

- [AEK<sup>+</sup>17] Henry Adams, Tegan Emerson, Michael Kirby, Rachel Neville, Chris Peterson, Patrick Shipman, Sofya Chepushtanova, Eric Hanson, Francis Motta, and Lori Ziegelmeier. Persistence Images: A Stable Vector Representation of Persistent Homology. *Journal of Machine Learning Research*, 18(8):1–35, 2017.
- [BCR84] Christian Berg, Jens Christensen, and Paul Ressel. *Harmonic Analysis on Semigroups: Theory of Positive Definite and Related Functions*. Springer, 1984.
- [BL15] Ulrich Bauer and Michael Lesnick. Induced matchings and the algebraic stability of persistence barcodes. *Journal of Computational Geometry*, 6(2):162–191, 2015.
- [BLT09] Xiang Bai, Wenyu Liu, and Zhuowen Tu. Integrating contour and skeleton for shape classification. In *Proceedings of the 12th IEEE International Conference on Computer Vision*, pages 360 – 367, 11 2009.
- [Bub15] Peter Bubenik. Statistical Topological Data Analysis using Persistence Landscapes. *Journal of Machine Learning Research*, 16:77–102, 2015.
- [Car09] Gunnar Carlsson. Topology and data. *Bulletin of the American Mathematical Society*, 46:255–308, 2009.

- [CCO17] Mathieu Carrière, Marco Cuturi, and Steve Oudot. Sliced Wasserstein Kernel for Persistence Diagrams. In *Proceedings of the 34th International Conference on Machine Learning*, 2017.
- [CdSGO16] Frédéric Chazal, Vin de Silva, Marc Glisse, and Steve Oudot. *The Structure and Stability of Persistence Modules*. Springer, 2016.
- [COO15] Mathieu Carrière, Steve Oudot, and Maks Ovsjanikov. Stable Topological Signatures for Points on 3D Shapes. *Computer Graphics Forum*, 34, 2015.
- [CSEH07] David Cohen-Steiner, Herbert Edelsbrunner, and John Harer. Stability of Persistence Diagrams. *Discrete and Computational Geometry*, 37(1):103–120, 2007.
- [dFF15] Barbara di Fabio and Massimo Ferri. Comparing persistence diagrams through complex vectors. *CoRR*, abs/1505.01335, 2015.
- [EH10] Herbert Edelsbrunner and John Harer. *Computational Topology: an introduction*. AMS Bookstore, 2010.
- [GZZ10] Zhenhua Guo, Lei Zhang, and David Zhang. A completed modeling of local binary pattern operator for texture classification. *IEEE Transaction on Image Processing*, pages 1657–1663, 2010.
- [Hei01] Juha Heinonen. *Lectures on Analysis on Metric Spaces*. Springer, 2001.
- [HKNU17] Christoph Hofer, Roland Kwitt, Marc Niethammer, and Andreas Uhl. Deep Learning with Topological Signatures. In *Advances in Neural Information Processing Systems 30*, pages 1633–1643. Curran Associates, Inc., 2017.
- [KFH16] Genki Kusano, Kenji Fukumizu, and Yasuaki Hiraoka. Persistence Weighted Gaussian Kernel for Topological Data Analysis. In *Proceedings of the 33rd International Conference on Machine Learning*, pages 2004–2013, 2016.
- [KFH17] Genki Kusano, Kenji Fukumizu, and Yasuaki Hiraoka. Kernel method for persistence diagrams via kernel embedding and weight factor. *CoRR*, abs/1706.03472, 2017.
- [Kön86] Hermann König. *Eigenvalue Distribution of Compact Operators*. Operator Theory: Advances and Applications. Birkhäuser, 1986.
- [OMP<sup>+</sup>02] Timo Ojala, Topi Mäenpää, Matti Pietikäinen, Jaakko Viertola, Juha Kyllönen, and Sami Huovinen. Outex - new framework for empirical evaluation of texture analysis algorithms. In *Proceedings of the 16th International Conference on Pattern Recognition*, pages 701–706, 2002.
- [Oud15] Steve Oudot. *Persistence Theory: From Quiver Representations to Data Analysis*. Number 209 in Mathematical Surveys and Monographs. American Mathematical Society, 2015.
- [RHBK15] Jan Reininghaus, Stefan Huber, Ulrich Bauer, and Roland Kwitt. A Stable Multi-Scale Kernel for Topological Machine Learning. In *IEEE Conference on Computer Vision and Pattern Recognition*, 2015.
- [Rob10] James C. Robinson. *Dimensions, Embeddings, and Attractors*, volume 186 of *Cambridge Tracts in Mathematics*. Cambridge University Press, 2010.
- [SP04] Robert Sumner and Jovan Popović. Deformation transfer for triangle meshes. *ACM Transactions on Graphics*, 23(3):399–405, 2004.
- [SS12] Ingo Steinwart and Clint Scovel. Mercer’s theorem on general domains: on the interaction between measures, kernels, and RKHSs. *Constructive Approximation*, 35:363–417, 2012.
- [TMMH14] Katharine Turner, Yuriy Mileyko, Sayan Mukherjee, and John Harer. Fréchet Means for Distributions of Persistence Diagrams. *Discrete and Computational Geometry*, 52(1):44–70, 2014.
- [Ver16] Sara Kalisnik Verovsek. Tropical Coordinates on the Space of Persistence Barcodes. *CoRR*, abs/1604.00113, 2016.